http://dx.doi.org/10.5012/bkcs.2014.35.1.69

Characterization of Fly Ash by Field-Flow Fractionation Combined with SPLITT Fractionation and Compositional Analysis by ICP-OES

Dong Young Kang, Chul Hun Eum,†,* and Seungho Lee‡

Yonsei Center for Research Facilities, Seoul 120-749, Korea
*†Korea Institute of Geoscience and Mineral Resources, Daejeon 305-350, Korea. *E-mail: cheum@kigam.re.kr*
‡Department of Chemistry, Hannam University, Daejeon 305-811, Korea
Received September 12, 2013, Accepted October 6, 2013

Accurate analysis of fly ash particles is not trivial because of complex nature in physical and chemical properties. SPLITT fractionation (SF) was employed to fractionate the fly ash particles into subpopulations in large quantities. Then the SF-fractions were analyzed by the steric mode of sedimentation field-flow fractionation (Sd/StFFF) for size analysis. The SF-fractions were also analyzed by ICP-OES. The results showed that the fly ash is mainly composed of Fe, Ca, Mg and Mn. No particular trends were observed between the particle size and the concentrations of Fe, Ca, Mg, while Mn, Cu and Zn were in higher concentrations in smaller particles. Sample preparation procedures were established, where the fly ash particles were sieved to remove large contaminants, and then washed with acetone to remove organics on the surface of particles. The sample preparation and analysis methods developed in this study could be applied to other environmental particles.

Key Words : Fly ash, Field-flow fractionation, SPLITT fractionation, Characterization

Introduction

Fly ash is a major component of the combustion product (usually 60 to 88%) emitted by burning of pulverized coal from thermo-electric power stations.[1,2] Being generated from various constituents in the coals, fly ash is a complex mixture of inorganic and organic compounds having heterogeneous physicochemical properties. Fly ash is composed of particles of various sizes ranging from less than nanometers up to a few micrometers. Fly ash may contain heavy metals and toxic organic compounds such as polycyclic aromatic hydrocarbon (PAH), polychlorinated biphenyls (PCBs) and polychlorinated dibenzodioxins (PCDDs),[3,4] which are easily leached out into environment.[4-9] Recent study of epidemiology has shown that increased concentration of airborne particles was related to increased mortality and morbidity from respiratory and cardiovascular diseases.[10-12] Most thermo-electric power stations are now equipped with electrostatic precipitators to reduce emission of fly ash.[2]

There have been reports on the relationship between the particle size of the fly ash and its chemical composition.[2-4,11,13-23] Generally the metal content tends to increase as the particle size decreases. This dependency is prominent for particles smaller than 50 μm and for the more volatile metals such as Pb, Cu, Cd, As, Zn, *etc*.[20,21,24] This increase in the metal content is likely due to increased surface area with decreasing particle size. Analysis of particle size distribution of fly ash is thus important for understanding of the environmental effect of fly ash. Although there have been numerous reports on the size analysis of fly ash particles and on the analysis of the trace elements associated with the fly ash, the relationship between the particle size and the chemical composition has not yet been thoroughly investigated.[11,16,17]

Split-flow thin (SPLITT) cell fractionation (SF) is a technique that can be used for fractionation of colloids and particulate materials in a preparative scale.[25-29] SF generally provides a binary separation (fractionation into two sub-populations) in one operation.

Figure 1 shows a schematic view of SF channel operating in the full-feed depletion (FFD) mode,[30-32] where, unlike in a conventional mode, the bottom inlet (inlet b') is blocked, and only the top inlet (inlet a') is used for feeding of the sample suspension. The sample particles settle while being transported down the channel toward the outlet. Particles settling fast enough to cross the outlet splitting plane (OSP) will exit through the bottom outlet (outlet b), and the others will exit through the top outlet (outlet a), thus yielding a binary separation of the sample. SF is non-destructive as the sample components are under little mechanical stress, if any, during

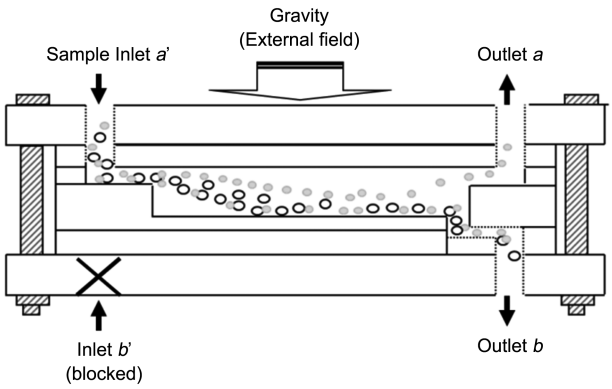

Figure 1. Schematic view of SF channel operating in full-feed depletion (FFD) mode.

SF operation. And the separation is tunable that the cut-off diameter (d_c) is readily controlled by varying the ratio of outlet flow rates, which affects the vertical position of OSP in the channel.

Field-flow fractionation (FFF) is a family of elution-based separation techniques applicable to various types of macromolecules and colloidal particles ranging in sizes from a few nanometers up to about 100 μm.[33] FFF has been used to separate biological, pharmaceutical, environmental, food, and industrial materials.[14,33-41] Unlike most chromatography columns, FFF channel is open (unpacked), wherein a laminar flow having a parabolic flow profile transports the components down the channel.

In this study, sedimentation FFF (SdFFF) was employed to characterize the size distributions of SF fractions of fly ash. And then their chemical compositions were analyzed using inductively coupled plasma-optical emission spectrometry (ICP-OES) and energy dispersive X-ray spectroscopy (EDX). Then the relationship between the chemical composition and the particle size was studied.

Theory

In the FFD mode of SF (FFD-SF), the cutoff diameter (dc) is given by[30,42]

$$d_c = \sqrt{\frac{18\eta}{b\,L\,G\,\Delta\rho}(\dot{V}(a') - \dot{V}(b'))} \quad (1)$$

where $\dot{V}(a)$ and $\dot{V}(a')$ are the volumetric flow rate at the outlet a and the inlet a', respectively, η the viscosity of carrier liquid, b the channel breadth, L the channel length, G the gravity, and $\Delta\rho$ is the density difference between the particle and the carrier liquid.

The resolution in FFD-SF may not be as high as that in the conventional mode due to the lack of the bottom inlet flow. Some of particles smaller than d_c may exit through the outlet b, contaminating the SF fraction collected from the outlet b (SF fraction-b).[30,43] This is because there is no incoming flow through the inlet b' to push the sample particles toward the upper wall of the channel to form a narrow sample layer. Still, the FFD mode provides an attractive alternative to the conventional mode as it does not cause dilution of the sample, which is particularly useful when the particle content in the sample is very low such as many environmental particles or when the SF fractions are to be subjected to other analysis such as ICP-OES or AAS, etc. In the conventional mode of SF (where both inlets are used), the flow rate through the inlet b' is usually much higher than that through the inlet a' (usually about 10 times), resulting in about 10 times dilution of the sample after SF operation. The contamination of the fraction b in the FFD mode could be reduced by repeating SF operation on the fraction-b (re-feeding of the fraction-b).

Also, in FFD-SF, a flow-splitter is not needed at the channel inlet, allowing the SF channel to be lager, which, in turn, allows higher throughput (the amount of the sample that can be treated by SF in a given time period). Usually the size of the SF channel is limited due to the presence of the flow-splitter, which may be distorted if the channel size exceeds a certain limit.

In the steric mode of SdFFF, the retention time (t_r) of a particle is related with the particle diameter (d) by[44]

$$t_r = \frac{wt^o}{3\gamma d} \quad (2)$$

where w is the channel thickness, t^o the channel void time, and γ a dimensionless "steric correction factor." It can be seen that, as the particle size increases, the retention time decreases (larger particles are eluted faster).

Due to an uncertainty in γ,[45] the size determination by Sd/StFFF requires a calibration using a plot of log t_r *vs.* log d, which is often expressed by[46]

$$\log t_r = -S_d \log d + \log t_{r1} \quad (3)$$

where S_d is the diameter-based selectivity (typically in the range of 0.7-0.8), and t_{r1} a constant equal to the extrapolated value of the retention time of particles of unit diameter.

If γ is constant, this plot is expected to be a linear.

The mass-based particle size distribution, $m(d)$, which represents the relative mass as a function of diameter, is then obtained by[47]

$$m(d) = c(t_r)\dot{V}\left|\frac{dt_r}{dd}\right| = c(t_r)\dot{V}\,S_d t_{r1}\left(\frac{t_r}{t_{r1}}\right)^{(S_d+1)/S_d} \quad (4)$$

where $c(t_r)$ is the detector signal at the retention time t_r, and $\dot{V}$ the volumetric flow rate. If the signal in Eq. (4) is divided by d^2, the mass-based size distribution is converted to the number-based size distribution.

Experimental

Sample Preparation. Fly ash was collected using an electrostatic precipitator equipped in a thermo-electric power plant in Dang-Jin, Korea. Fly ash were recovered from the storage bag, and then dried in an oven at 105 °C for 2 h. For accurate SF and FFF analysis, the fly ash particles need to be well suspended in the aqueous medium. The fly ash powder was first washed with acetone to remove the organic compounds that may exist on the surface of the particles, which could cause particle aggregation.[41] About 25 mL of acetone was added to 3-5 g of dry fly ash powder and then the mixture was vortexed for 3 min. The mixture was then centrifuged at 200 rpm for another 3 min. After removing the supernatant, the same amount of acetone was added again for another washing. After the acetone-washing, the fly ash was washed with water three times in the same manner (about 50 mL of water was used at a time). The wet fly ash was dispersed in the carrier liquid (water with 3% FL-70), and then passed through a 220-mesh sieve (~44 μm in pore size) to remove large particles. The densities of fly ash particles vary, and in this study, the average density of 2.5 g/mL was chosen for d_c calculation.[40]

For ICP-OES analysis, SF fractions were filtered through a 0.45 μm membrane filter (MFS, Advantec, Inc., Tokyo, Japan) to collect the particles. The particles were dried in an oven at 105 °C for 2 h together with the filter paper. The fly ash particles dried in the filter were placed in a ceramic crucible and ashed in a furnace at 750 °C for 2.5 h. After the ashing, the fly ash were weighed, and then dissolved in 5 mL of 12 M HCl in a 50 mL Pt crucible. After adding 2 mL of $HClO_4$ (for wet-combustion) and 5 mL of HF (to dissolve silica), the Pt crucible was slowly heated on a hot plate for 5 h at 240 °C until the mixture is completely dried. Finally 5 mL of HCl and 45 mL of water were added to dissolve the dried solid for ICP-OES analysis.

SF Fractionation. A new large scale SF channel was assembled for this study, which was designed to operate only in the FFD mode.[48] The SF channel was 50 cm long, 10 cm wide and 1,700 ìm thick. The inlet flow (sample-feeding flow) was provided by a Masterflex peristaltic pump (Barrant, BT, USA). The two outlet flow rates, $V(a)$ and $V(b)$, were controlled by connecting tubings of various diameters and lengths to the outlets.

The carrier fluid was water containing 3% (w/v) of FL-70 (Fisher Scientific, Fair Lawn, NJ, USA). For the calculation purposes, viscosity and density of the carrier liquid are assumed to be 0.01 poise and 1.00 g/mL, respectively. The SF system was maintained at room temperature during operation.

SdFFF. The SdFFF channel used in this study is 0.019 cm thick, 89.5 cm long and 1.5 cm wide. The radius of the channel rotor is 15.1 cm. The channel surface was a polished Hestalloy-C alloy which is consisted of 56% Ni, 15% Cr, 17% Mo, 5% Fe, 4% W and traces of Mn and Si. The channel void volume was 2.8 mL when measured from the elution volume of bromo phenol blue (BPB). The carrier liquid was pumped by a M930 HPLC pump (Young-Lin Scientific Co., Anyang, Korea). The eluted particles were monitored by a Gilson Model UV-112 detector operating at the fixed wavelength of 254 nm. The control and data collection of the SdFFF system was performed by a personal computer equipped with the Lab View (National instrument Co., Austin, Texas, USA). The sample was injected directly into the channel through a rubber septum, and the injection volume was between 20 and 100 μL depending on the sample concentration. All SdFFF experiments were performed at room temperature (23-24 °C), and the carrier liquid was water with 3% FL-70 and 0.02% NaN_3.

Optical Microscopy (OM). The optical microscopy (OM) was performed by using an Olympus BX51TF optical microscopy (Shinjuku Monolith, Shinjuku-ku, JAPAN). For all OM analysis of the size distribution of the fly ash particles were measured by using the Image Inside software (Focus, Daejeon, Korea).

Photon-Correlation Spectrometry (PCS). The PCS was performed by using a Zeta Sizer-3000HSA (Malvern, UK) to determine size distributions of fly ash particles.

ICP-OES. A Perkin Elmer Optima 5300 DV ICP-OES (Norwalk, CT, USA) was used for elemental analysis of the fly ash. For analysis of SdFFF slices or the SF fractions, the samples were filtered through a 0.45 μm filter and dried.

SEM-EDX. A Hitachi S-5500 (Tokyo, Japan) field emission scanning electron microscope (FE-SEM) was used to analyze the fly ash at the acceleration potential of 30 keV (resolution = 0.4 nm) and Energy dispersive X-ray spectrometer (EMAX, HORIBA) was used to analyze chemical compositions of fly ash at detectable range of ^{4}Be-^{92}V.

Results and Discussion

Size Distribution of Fly Ash before and after the Acetone Washing. Fly ash particles may contain some organic compounds on surface, which could cause particle aggregation. If present, the aggregated particles need to be disintegrated for reliable and reproducible size data from SdFFF analysis. Figure 2 shows size distributions of fly ash obtained by OM and SdFFF before and after the acetone washing.

For size measurements, the fly ash dispersion was allowed to settle for 10 min, and then the supernatant was taken for size analysis. As shown in Figure 2, large particles disappear after the acetone washing, probably due to disaggregation of the particles by the removal of the organic compounds adsorbed on the surface of the particles.

Figure 3 show size distributions of the same fly ash obtained by PCS (dotted lines) and SdFFF (lines). The SdFFF data shown in Figure 3 are the same as those shown in Figure 2. PCS results also show reduction in size by acetone washing. It is noted that the size from PCS are much lower than those from SdFFF, probably due to settling of larger particles during 3 min PCS measurements. It seems PCS is not adequate for size measurement of large and dense particles such as fly ash.

Size-based Separations of Fly Ash by SdFFF. After the sieving and acetone-washing, the fly ash suspension was analyzed by the steric mode of SdFFF (Sd/StFFF).

Figure 4 shows a Sd/StFFF fractogram of the fly ash and OM pictures of four slices of the fractogram. The OM pictures show that SdFFF provides a size-based separation of the fly ash particles, where larger particles are eluted earlier than

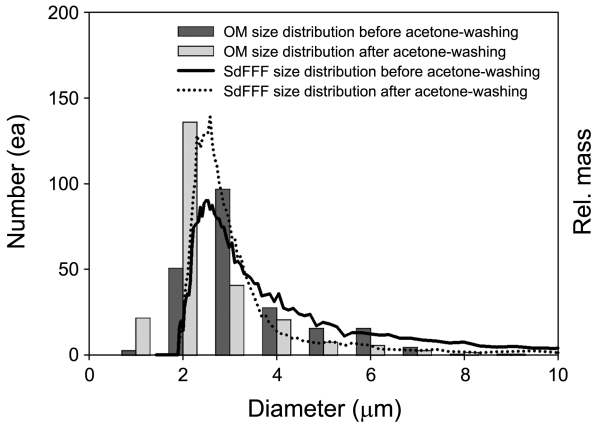

Figure 2. Size distributions of fly ash determined by OM (bars) and SdFFF (lines) before and after acetone washing. The SdFFF channel rotation rate was 190 rpm, and flow rate was 5 mL/min.

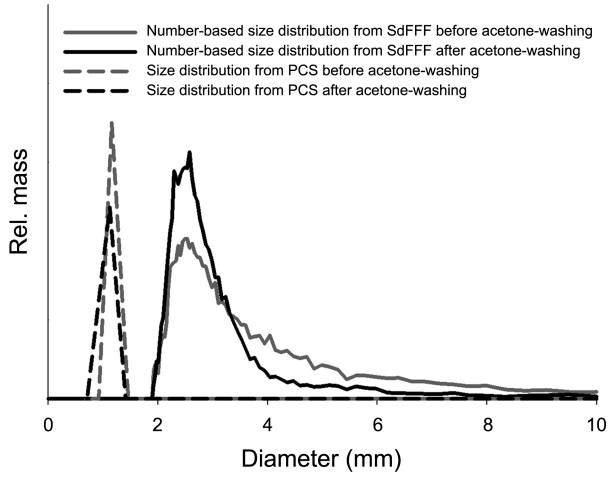

Figure 3. Size distributions of fly ash obtained before and after acetone-washing by PCS (dotted lines) and SdFFF (solid lines). SdFFF conditions were the same as those in Figure 2.

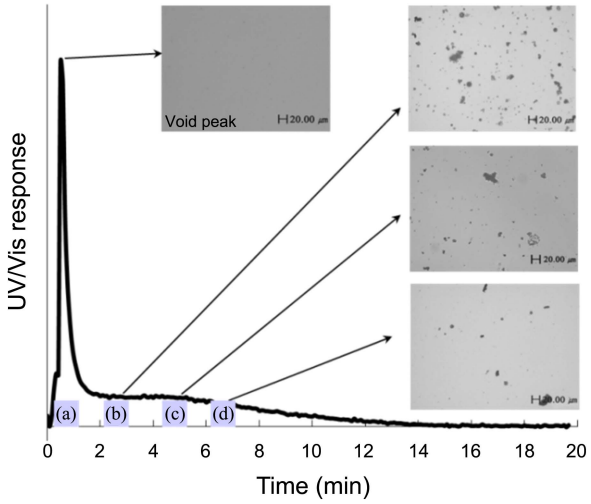

Figure 4. Sd/StFFF fractogram of fly ash and OM (× 200) pictures of four fractions. SdFFF conditions were the same as those in Figure 2.

the smaller ones. The slice-A is the void peak, and contains unretained small particles that could not be recognized by OM.

SF Fractionation of Fly Ash. SF was employed to obtain size-fractions of the fly ash in large quantities. Figure 5 shows the procedure used in this study for size-based fractionation by SF, followed by Sd/StFFF analysis. After the sieving and acetone washing, the fly ash particles were fractionated by SF. The SF fraction-*a* and *b* obtained by FFD-SF were analyzed by SdFFF and SEM-EDX. The fraction-*b* was fractionated again by FFD-SF at the same condition to produce the fractions-*ba* and *bb*, which were analyzed again by Sd/StFFF.

Figure 6 shows optical micrographs of the fly ash particles in the SF fractions obtained by the procedure shown in Figure 5. The total mass of particles in the fly ash suspension fed into the SF channel was 3 g, and those in the fractions-*a*

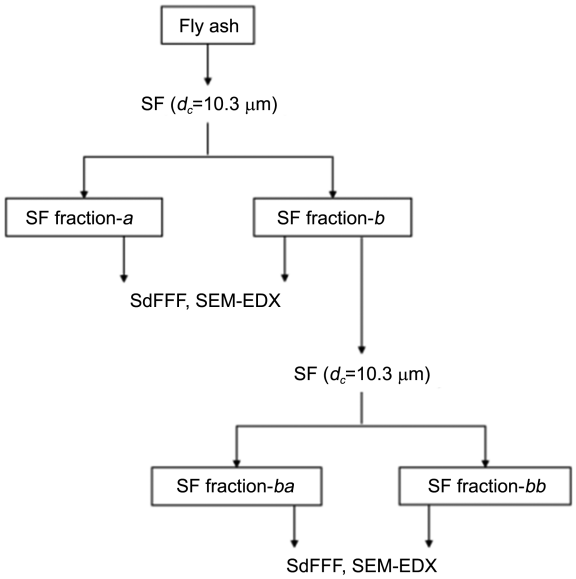

Figure 5. Procedure for SF fractionation of fly ash followed by SdFFF analysis of SF fractions.

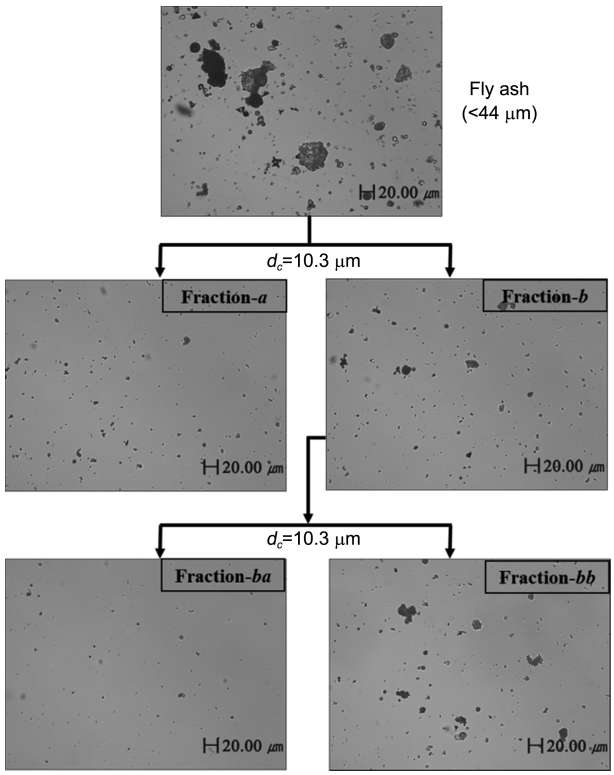

Figure 6. Optical micrographs (× 200) of SF fractions of fly ash.

and *b* were 0.757 and 1.986 g, respectively. The sample feeding flow rate was 118 mL/min, and the outlet flow rates, $V(a)$ and $V(b)$ were 24 and 94 mL/min, respectively. The cut-off diameter, d_c was 10.3 μm. As shown in Figure 6, a reasonable fractionation of fly ash particles were obtained with the fractions-*a* and *ba* containing mostly particles smaller than about 10 μm. Particles larger than about 10 μm were found only in the fractions-*b* and *bb*. The fractions-*b*

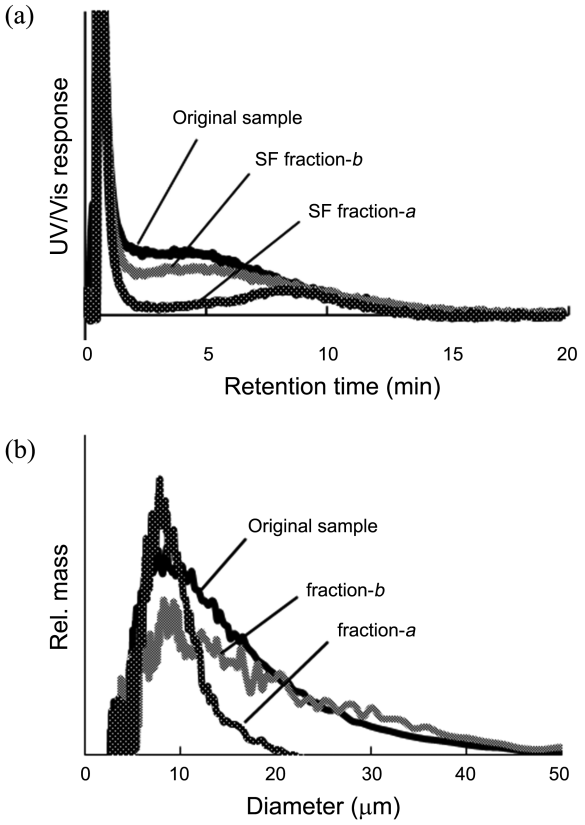

Figure 7. SdFFF fractograms (a) and size distributions (b) of fly ash in SF fractions-*a* and *b*. SdFFF conditions were the same as those in Figure 2.

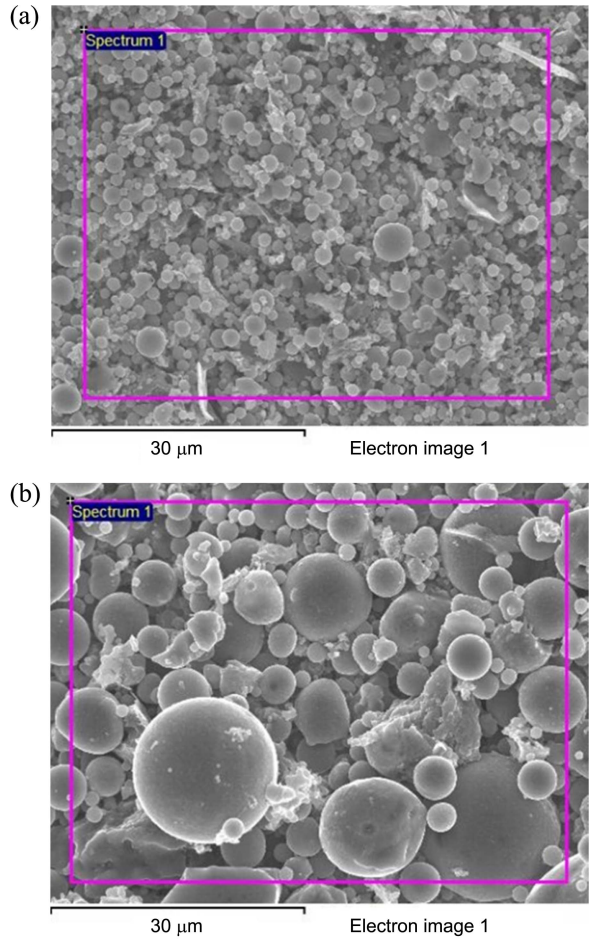

Figure 8. SEM images of SF fraction-*a* (a) and *b* (b).

and *bb* also contain particles smaller than d_c, which is expected by theory as mentioned earlier.

Sd/StFFF of SF Fractions. The SF fractions shown in Figure 6 were analyzed by Sd/StFFF. Figure 7(a) shows Sd/StFFF fractograms of fly ash in the original sample and the SF fractions-*a* and *b*, and Figure 7(b) the size distributions obtained from the fractograms shown in Figure 7(a). SdFFF conditions were the same as those in Figure 2. As shown in Figure 7(b), FFD-SF yielded fractionation of the fly ash particles into two subpopulations of different sizes with the fraction-*a* containing smaller particles and the fraction-*b* containing relatively larger particles.

Figure 8 shows SEM images of SF fractions-*a* (a) and *b* (b). As expected from Figure 7, the SF fraction-*a* mostly contains particles smaller than the cut-off diameter (d_c = 10.3 μm). As was observed in Figure 6, particles larger than about 10 ìm were found only in the fractions-*b* and *bb*, and the fractions-*b* and *bb* contain some particles smaller than d_c.

Figure 9(a) shows Sd/StFFF fractograms of fly ash in the SF fractions-*b*, *ba*, and *bb*, and Figure 9(b) the size distributions obtained from the fractograms shown in Figure 9(a). SdFFF conditions were again the same as those in Figure 2. Results shown in Figure 9 are similar with those shown in Figure 7. Compared to the fractogram of the fraction-*b*, the fractogram of the fraction-*ba* was shifted right, while that of the fraction-*bb* was shifted left, indicating the fraction-*b* was further separated after repeated SF operation. It is also noted that the size distributions of the fractions-*ba* and *bb* are narrower than that of the fraction-*b*. Results shown in Figures 6, 7, 8 and 9 clearly demonstrate the usefulness of SF in pre-fractionation of fly ash particles before SdFFF analysis.

ICP-OES Analysis of SF Fractions. Concentrations of various elements in the fly ash particles in SF fractions were measured by ICP-OES, and the results are shown in Table 1. For most elements shown in Table 1, the concentrations are higher in the fraction-*a* than those in the fraction-*b*, as expected, because the fraction-*a* contains relatively smaller particles. Generally the concentrations of the elements adsorbed on particles are inversely proportional to the particle size as the surface area increases with decreasing size. It is noted that measured element concentrations shown in Table 1 are for the entire particles, not just for those on the surface of the particles.

Results from ICP-OES indicate that the major elements of the fly ash particles are Fe, Ca, and Mg, for which no significant differences in concentrations were observed between the SF fraction-*a* than in *b*. Other elements show higher relative differences between concentration in the SF fraction-*a* than in *b*, suggesting they are absorbed on the surface of the particles from air during coal combustion and hence show higher concentration in the SF fraction-*a* than in *b*.[49] These

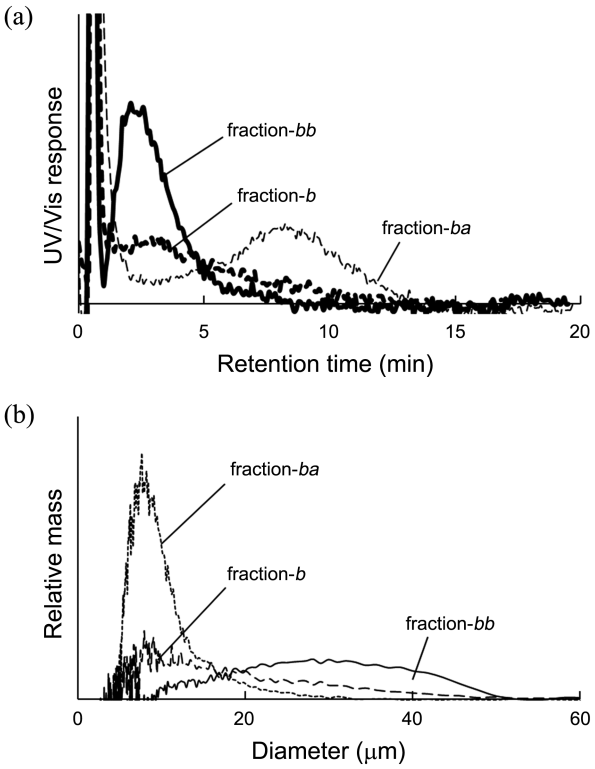

Figure 9. SdFFF fractograms (a) and size distributions (b) of fly ash in SF fractions-*b*, *ba* and *bb*. SdFFF conditions were the same as those in Figure 2.

Table 1. Chemical composition of fly ash in SF fractions-*a* and *b* determined by ICP-OES

Element	Element concentration (mg/L) in (n=3)	
	Fraction-*a*	Fraction-*b*
Fe	44.4 (±1.8)	44.4 (±1.8)
Ca	15.6 (±0.5)	15.1 (±0.5)
Mg	5.95 (±1.8)	4.75 (±1.8)
Mn	0.52 (±0.02)	0.32 (±0.01)
Zn	0.37 (±0.01)	0.15 (±0.01)
Cr	0.17 (±0.01)	0.09 (±0.01)
Cu	0.17 (±0.02)	0.10 (±0.01)
Cd	< 0.01	<0 .01

results are similar with the results reported in a previous report.[16]

Table 2 shows elemental composition determined by SEM-EDX. The results show the surface of the fly ash particles are mainly composed of elements such as C, O, Mg, Al, Si, K, Ca, Ti and Fe. Smaller particles (SF fraction-*a*) contain higher concentrations of C, Al, Si, Ca and Fe than larger ones, while larger particles contain higher concentration of O, Mg, K, and Ti. Carbon content is higher in the SF fraction-*a* (smaller particles), which originate from incomplete combustion of the lignite.[18] The results obtained for Ti and K are similar with the results reported elsewhere.[49]

It can be seen that the SEM-EDX results are somewhat different from those in Table 1. First, SEM-EDX measures the relative elemental composition on the particle surface, not the bulk of the particles. The difference also comes from the differences in the sample preparation procedures. For ICP-OES analysis, carbon was not included because carbon is not dissolved in acid. Unlike SEM-EDX, the ICP-OES analysis yields the composition of entire particles, and thus the results from ICP-OES do not explain much on the adsorption of various toxic organic and inorganic compounds. It is recommended that a proper analysis method must be chosen based on the type of information needed.

Table 2. Chemical Composition of fly ash in SF fractions-*a* and *b* determined by SEM-EDX

Element	Weight % in (n=3)	
	Fraction-*a*	Fraction-*b*
C	24.70	12.84
O	43.64	50.05
Mg	0.29	0.35
Al	10.50	0.26
Si	14.91	12.52
K	0.53	18.60
Ca	0.84	0.73
Ti	0.88	1.00
Fe	3.71	0.62
Total	100.00	100.00

Conclusion

Results shown in this study suggest that SF can provide a useful tool for pre-separation of complex particles such as the fly ash before characterization by SdFFF or other elemental analysis.

Acknowledgments. This research was supported by the Basic Research Project of The Korea Institute of Geoscience and Mineral Resources (KIGAM). This work was also supported by the Hannam University.

References

1. Vassilev, S. V.; Vassileva, C. G. *Fuel* **2007**, *86*, 1490.
2. Iordanidis, A.; Buckman, J.; Triantafyllou, A. G.; Asvesta, A. *Int. J. Coal Geol.* **2008**, *73*, 63.
3. Lu, S. Y.; Du, Y.; Yan, J. H.; Li, X. D.; Ni, M. J.; Cen, K. F. *J. Air Waste Manage. Assoc.* **2012**, *62*, 717.
4. Kurokawa, Y.; Takahiko, M.; Matayoshi, N.; Satoshi, T.; Kazumi, F. *Chemosphere* **1998**, *37*, 2161.
5. Tan, Z.; Xiao, G. *Waste Manage. Res.* **2012**, *30*, 285.
6. Gori, M.; Pifferi, L.; Sirini, P. *Waste Manage. (Oxford)* **2011**, *31*, 1514.
7. Kaupp, H.; Towara, J.; McLachlan, M. S. *Atmos. Environ.* **1994**, *28*, 585.
8. Cao, S. S.; Wu, G. H.; Su, R. X. *Huanjing Kexue/Environmental Science* **2011**, *32*, 1831.
9. Qian, L.; Ma, M.; Cheng, D. *J. Radioanal. Nucl. Chem.* **2012**, 1.
10. Jones, T.; Blackmore, P.; Leach, M.; BéruBé, K.; Sexton, K.; Richards, R. *Environ. Monit. Assess.* **2002**, *75*, 293.

11. Natusch, D. F. S.; Wallace, J. R.; Evans, C. A. *Science* **1974**, *183*, 202.
12. Dwivedi, S.; Saquib, Q.; Al-Khedhairy, A. A.; Ali, A. Y. S.; Musarrat, J. *Sci. Total Environ.* **2012**, *437*, 331.
13. Cuddihy, R. G.; Griffith, W. C.; McClellan, R. O. *Environ. Sci. Technol.* **1984**, *18*, 14A.
14. Hassellöv, M.; Lyvén, B.; Beckett, R. *Environ. Sci. Technol.* **1999**, *33*, 4528.
15. Murphy, D. M.; Garbarino, J. R.; Taylor, H. E.; Hart, B. T.; Beckett, R. *J. Chromatogr. A* **1993**, *642*, 459.
16. Furuya, K.; Miyajima, Y.; Chiba, T.; Kikuchi, T. *Environ. Sci. Technol.* **1987**, *21*, 898.
17. Conzemius, R. J.; Welcomer, T. D.; Svec, H. J. *Environ. Sci. Technol.* **1984**, *18*, 12.
18. Vassilev, S. V.; Vassileva, C. G. *Fuel Process. Technol.* **1996**, *47*, 261.
19. Kostova, I.; Vassileva, C.; Hower, J.; Mastalerz, M.; Vassilev, S.; Nikolova, N. *Comptes Rendus de L'Academie Bulgare des Sciences* **2011**, *64*, 253.
20. Koukouzas, N.; Ketikidis, C.; Itskos, G. *Fuel Process. Technol.* **2011**, *92*, 441.
21. Yanlong, L.; Rundong, L.; Zhihui, Z.; Haijun, Z.; Lei, W.; Jingde, L. In *Effect of Particle Size on the Speciation Distribution of Heavy Metals in MSWI Fly Ash*, Intelligent Computation Technology and Automation (ICICTA), 2011 International Conference on, 28-29 March 2011; 2011; pp 824-827.
22. Sánchez de la Campa, A. M.; Moreno, T.; de la Rosa, J.; Alastuey, A.; Querol, X. *J. Hazard. Mater.* **2011**, *190*, 713.
23. Zhang, T. S.; Yu, Q. J.; Wei, J. X.; Zhang, P. P. *Adv. Cem. Res.* **2011**, *23*, 299.
24. Liu, S. C.; Jiang, C. S.; Hao, Q. J.; Li, Q. L.; Shi, Y. *Adv. Mat. Res.* **2012**, *414*, 166.
25. Dondi, F.; Contado, C.; Blo, G.; Garçia Martin, S., *Chromatographia* **1998**, *48*, 643.
26. Gao, Y.; Myers, M. N.; Barman, B. N.; Giddings, J. C. *Part. Sci. Technol.* **1991**, *9*, 105.
27. Springston, S. R.; Myers, M. N.; Giddings, J. C. *Anal. Chem.* **1987**, *59*, 344.
28. Giddings, J. C. *Sep. Sci. Technol.* **1985**, *20*, 749.
29. Giddings, J. C. *Sep. Sci. Technol.* **1992**, *27*, 1489.
30. Contado, C.; Dondi, F.; Beckett, R.; Giddings, J. C. *Anal. Chim. Acta* **1997**, *345*, 99.
31. Lee, S.; Cho, S. K.; Yoon, J. W.; Choi, S. H.; Chun, J. H.; Eum, C. H.; Kwen, H. *J. Liq. Chromatogr. Related Technol.* **2010**, *33*, 27.
32. Lee, S.; Lee, J. Y.; Lee, T. W.; Jung, E. C.; Cho, S. K. *Bull. Korean Chem. Soc.* **2011**, *32*, 4291.
33. Giddings, J. C., Field-Flow Fractionation. *Chem. Eng. News* 1988; pp 34-45.
34. Stevenson, S. G.; Ueno, T.; Preston, K. R. *Anal. Chem.* **1998**, *71*, 8.
35. Fraunhofer, W.; Winter, G.; Coester, C. *Anal. Chem.* **2004**, *76*, 1909.
36. Arfvidsson, C.; Wahlund, K.-G. *J. Chromatogr. A* **2003**, *1011*, 99.
37. Nilsson, M.; Birnbaum, S.; Wahlund, K.-G. *J. Biochem. Bioph. Methods* **1996**, *33*, 9.
38. Petteys, M. P.; Schimpf, M. E. *J. Chromatogr. A* **1998**, *816*, 145.
39. Ranville, J. F.; Chittleborough, D. J.; Shanks, F.; Morrison, R. J. S.; Harris, T.; Doss, F.; Beckett, R. *Anal. Chim. Acta* **1999**, *381*, 315.
40. Kim, W.-S.; Lee, D. W.; Lee, S. *Anal. Chem.* **2002**, *74*, 848.
41. Eum, C. H.; Kang, D. Y.; Lee, T. W.; Lee, S. *Anal. Sci. Technol.* **2009**, *22*, 75.
42. Fuh, C. B.; Myers, M. N.; Giddings, J. C. *Ind. Eng. Chem. Res.* **1994**, *33*, 355.
43. Blo, G.; Contado, C.; Grandi, D.; Fagioli, F.; Dondi, F. *Anal. Chim. Acta* **2002**, *470*, 253.
44. Giddings, J. C. *Sep. Sci. Technol.* **1978**, *13*, 241.
45. Peterson, R. E.; Myers, M. N.; Giddings, J. C. *Sep. Sci. Technol.* **1984**, *19*, 307.
46. Giddings, J. C.; Moon, M. H.; Williams, P. S.; Myers, M. N. *Anal. Chem.* **1991**, *63*, 1366.
47. Moon, M. H.; Lee, S. *J. Microcolumn Sep.* **1997**, *9*, 565.
48. Lee, S.; Lee, T. W.; Cho, S. K.; Kim, S. T.; Kang, D. Y.; Kwen, H.; Lee, S. K.; Eum, C. H. *Microchem. J.* **2010**, *95*, 11.
49. Linak, W. P.; Wendt, J. O. L. *Fuel Process. Technol.* **1994**, *39*, 173.